Transcriptomics reveals the mycoparasitic strategy of the mushroom *Entoloma abortivum* on species of the mushroom *Armillaria*

Running title: Mycoparasitism of *Entoloma abortivum*

Rachel A. Koch[1] and Joshua R. Herr[1,2,#]

[1]Department of Plant Pathology, University of Nebraska, Lincoln, NE 68503, USA;

[2]Center for Plant Science Innovation, University of Nebraska, Lincoln, NE 68588, USA;

[#]Correspondence: Joshua R. Herr (jherr@unl.edu)

Abstract word count (including abstract and importance): 363

Text word count: 4938

ABSTRACT

During mycoparasitism, a fungus—the host—is parasitized by another fungus—the mycoparasite . The genetic underpinnings of these relationships have been best characterized in Ascomycete fungi. However, within Basidiomycete fungi, there are rare instances of mushroom-forming species parasitizing the reproductive structures, or sporocarps, of other mushroom-forming species. One of the most enigmatic of these occurs between *Entoloma abortivum* and species of *Armillaria*, where hyphae of *E. abortivum* are hypothesized to disrupt the development of *Armillaria* sporocarps, resulting in the formation of carpophoroids. However, it remains unknown whether carpophoroids are the direct result of a mycoparasitic relationship. To address the nature of this unique interaction, we analyzed gene expression of field-collected *Armillaria* and *E. abortivum* sporocarps and carpophoroids. Transcripts in the carpophoroids are primarily from *E. abortivum*, supporting the hypothesis that this species is parasitizing *Armillaria*. Most notably, we identified differentially expressed *E. abortivum* β-trefoil-type lectins in the carpophoroid, which we hypothesize bind to *Armillaria* cell wall galactomannoproteins, thereby mediating recognition between the mycoparasite and the host. The most significantly upregulated *E. abortivum* transcripts in the carpophoroid code for oxalate decarboxylases—enzymes that degrade oxalic acid. Oxalic acid is a virulence factor in many plant pathogens, including *Armillaria* species, however, *E. abortivum* has evolved a sophisticated strategy to overcome this defense mechanism. The number of gene models and genes that code for carbohydrate-active enzymes in the *E. abortivum* transcriptome were reduced

compared to other closely related species, perhaps as a result of the specialized nature of this interaction.

IMPORTANCE

By studying fungi that parasitize other fungi, we can understand the basic biology of these unique interactions. Studies focused on the genetic mechanisms regulating mycoparasitism between host and parasite have thus far concentrated on a single fungal lineage within the Ascomycota. The work presented here expands our understanding of mycoparasitic relationships to the Basidiomycota, and represents the first transcriptomic study to our knowledge that examines fungal-fungal relationships in their natural setting. The results presented here suggest that even distantly related mycoparasites utilize similar mechanisms to kill their host. Given that species of the mushroom-forming pathogen *Armillaria* cause plant root-rot diseases in many agroecosystems, an enhanced understanding of this interaction may contribute to better control of these diseases through biocontrol applications.

INTRODUCTION

Fungal mycoparasitism is a nutritional strategy where a living fungus—the host—is parasitized by and acts as a nutrient source for another fungus—the mycoparasite. Certain species of fungi in the Hypocreales (Ascomycota) are among the best-studied mycoparasites. Perhaps the most well-known of these are species of *Trichoderma* and *Clonostachys rosea*, which have biocontrol activity against plant pathogenic species of *Botrytis*, *Fusarium*, *Pythium*, and *Rhizoctonia* (1, 2). Other fungal mycoparasites in the Hypocreales include *Tolypocladium* species, many of which are parasites on the reproductive structures, or sporocarps, of species in the genus *Elaphomyces* (Eurotiales, Ascomycota) (3), as well as *Escovopsis weberi*, which is a specialized necrotrophic parasite of fungal gardens of attine ants (4, 5).

Less studied examples of mycoparasitism involve mushroom-forming fungi that parasitize other mushroom-forming fungi. Fewer than 20 reported mushroom species are capable of engaging in this type of interaction, making it an incredibly rare phenomenon given the total number of mushroom-forming fungi (6, 7). Examples of this interaction include *Volvariella surrecta*, which fruits from the pileus of its host, *Clitocybe nebularis* (8), which appears to remain unaffected by its parasite (7). More commonly, though, mushroom mycoparasites deform host sporocarps and likely prevent the dispersal of their spores. *Pseudoboletus parasiticus* fruits from the sporocarps of *Scleroderma* species, which, after infection, are no longer able to mature and disperse their spores (9). *Psathyrella epimyces* causes the deformation of sporocarp tissue of its host, *Coprinus comatus* (10). Additionally, of the ten mushroom species in the genus

Squamanita, all are known to be parasites of sporocarps of species in the genera *Cystoderma*, *Galerina*, *Hebeloma*, and *Inocybe* (7).

One of the most commonly encountered putative mycoparasitic interactions between two mushrooms involves species of *Armillaria* (Fig. 1A) and *Entoloma abortivum* (Fig. 1B). *Entoloma abortivum* is often encountered fruiting in soil, humus, or decaying logs in deciduous woods (11), while *Armillaria* species are facultative necrotrophs that can cause root rot in forest and agronomic systems worldwide (12, 13). Traditionally, *E. abortivum* was thought to exist in two forms: the typical mushroom form, which has a gray stipe, gray pileus and pink gills (Fig. 1B), and the carpophoroid form, which is white, subglobose and lacks well-formed gills (Fig. 1C–D). The carpophoroid form has traditionally been assumed to be *E. abortivum* sporocarps that did not develop properly due to parasitism by *Armillaria* species (11). However, macro- and microscopic studies of carpophoroid field collections determined that carpophoroids actually represent malformed *Armillaria* sporocarps permeated by *E. abortivum* hyphae (14). Laboratory inoculation experiments showed that *E. abortivum* interacts with *Armillaria* sporocarps to disrupt their morphological development (14).

Whether carpophoroids are the result of a mycoparasitic relationship, where *E. abortivum* serves as the mycoparasite and *Armillaria* species serve as the host, remains unknown. In order to address this, we initiated a transcriptome study after we encountered all three components of this system fruiting in close proximity—carpophoroids and individual sporocarps of *E. abortivum* and *Armillaria*. For a mycoparasite to be successful, there are several crucial steps in the utilization of a fungal host for nutrition. These steps include: 1) sensing the host; 2) recognition and

attachment to host hypha; 3) initiating defense responses; and 4) the eventual demise of the host (15). Previous genomic and transcriptomic studies elucidated the genetic machinery that model mycoparasites utilize during each of these steps (15–17). In this work, we used transcriptomic and meta-transcriptomic techniques to analyze the genomic toolbox of *E. abortivum* and *Armillaria* during the carpophoroid stage. We show that the gene expression profiles of *E. abortivum* resemble those of known mycoparasitic species, as well as predict certain genes in both species that facilitate this interaction. Additionally, we used transcriptomic information to determine the species of *Armillaria* involved in this association.

RESULTS

Transcriptome assemblies of* Entoloma abortivum *and* Armillaria*. In order to benchmark gene diversity and baseline expression levels of the field-collected mushroom species in our study, we sequenced the sporocarp transcriptomes of *E. abortivum* and the *Armillaria* species found in close proximity to the carpophoroids. To date, there are several transcriptomic studies of *Armillaria* species (18, 19), but none for any *Entoloma* species. The assembled transcriptome of *E. abortivum* was just under 120 million base pairs. There were a total of 43,599 contigs and an N50 value of 3,527; 94.5% of benchmark universal single-copy orthologs (BUSCOs) from the Agaricales were present in the *E. abortivum* transcriptome. A large number of contigs represented duplicated gene models with potential splice variation. Within the contigs, a total of 9,728 unique gene models were recovered in the transcriptome assembly (Fig. 2) with 603 genes differentially expressed in the carpophoroid tissue and 403 genes

differentially expressed in the sporocarp tissue (Fig. 3). The transcriptome contained 195 genes that code for carbohydrate-active enzymes (CAZymes). The transcriptome lacks any genes that code for cellobiohydrolases (GH6 and GH7), xylanases (GH10, GH11, GH30) and auxiliary proteins like polysaccharide monooxygenases (GH61), but does contain nine chitinases (GH18) (Fig. 2). Genes detected in the *E. abortivum* transcriptome that might be important in mycoparasitic interactions include: ten putative secondary metabolite gene clusters, one G-coupled protein receptor (GCPR), 38 ATP-binding cassette (ABC) transporters and 113 genes from the major facilitator superfamily (MFS) (Fig. 3). The average gene expression (in normalized units of trimmed mean of m-values (TMM)) of the ten most highly expressed *E. abortivum* genes in the sporocarp ranged from 4,333 to 17,890. Information about the ten most highly expressed transcripts in the sporocarps is available in Table 1.

The assembled transcriptome of *Armillaria* was just over 138 million base pairs. There were a total of 63,905 contigs, an N50 value of 2,845, and 97.8% of the BUSCOs representative of the Agaricales were present in the transcriptome. Again, a large number of the contigs represented duplicated gene models with potential splice variation. A total of 38,215 unique gene models were recovered (Fig. 2) and 2,619 transcripts were differentially expressed in the carpophoroid tissue, whereas 9,820 were differentially expressed in the sporocarp tissue (Fig. 3). The transcriptome contained 580 genes that code for CAZymes, with 34 of those coding for chitinases (Fig. 2). Genes detected in the *Armillaria* transcriptome that might be important in mycoparasitic interactions include: 12 putative secondary metabolite gene clusters, five GCPRs, 59 ABC transporters and 144 MFS transcripts (Fig. 3). The average TMM of the ten most

161 highly expressed *Armillaria* genes in the sporocarp ranged from 8,438 to 36,477. The
162 most highly expressed gene was annotated as a cell wall galactomannoprotein (Fig. 4
163 and 5) (Table 2), while, notably, the fourteenth most highly expressed gene in the
164 sporocarp coded for isocitrate lyase (Table 2, Fig. 5).
165
166 **Metatranscriptomic analysis of combined fungal hyphae in carpophoroid tissue.**
167 We sequenced the metatranscriptome of the mixed tissue in the carpophoroids that are
168 typically found when *E. abortivum* and species of *Armillaria* are found in close proximity.
169 In the carpophoroid tissue, significantly more transcriptomic reads from *E. abortivum*
170 were identified than from *Armillaria* sp. ($t_{(8)}$ = 16.6, $p = 1.77\times10^{-7}$, n = 9 replicates per
171 species) (Fig. 6). The average number of *E. abortivum* mapped reads in the
172 carpophoroid tissue was 2,613,988, while the average number of *Armillaria* mapped
173 reads was 74,880 (Fig. 6). Multidimensional scaling (MDS) plots of *E. abortivum* (Fig.
174 7A) and *Armillaria* (Fig. 7B) show that the genetic distance between the *E. abortivum*
175 sporocarps and the carpophoroid is less than the distance between *Armillaria*
176 sporocarps and the carpophoroid.
177 The average TMM of the top ten most highly expressed *E. abortivum* genes in
178 the carpophoroid ranged from 9,075 to 68,720 (Table 1), while the average TMM of the
179 top ten most highly expressed *Armillaria* transcripts in the carpophoroid ranged from
180 300 to 9,049 (Table 2). The first and third most highly expressed *E. abortivum*
181 transcripts in the carpophoroid tissue code for two oxalate decarboxylases, both of
182 which were significantly differentially expressed in the carpophoroid tissue compared to
183 the sporocarp (Figs. 3, 4, 5 and Table 1). There were other differentially expressed *E.*

abortivum transcripts in the carpophoroid that were not as highly expressed that may also play a role in mycoparasitism. These include three β-trefoil-type lectins, three ABC transporters, two chitinases, and 14 MFS transcripts (Fig. 3, Table 1). No transcripts involved in secondary metabolite gene clusters were differentially expressed in the carpophoroids (Fig. 3). Opposingly, two *Armillaria* transcripts that code for putative senescence-associated proteins were significantly expressed in the carpophoroid compared to the sporocarp as well as a heat shock protein (Table 2).

Phylogenetic placement of* Armillaria *reads. Phylogenomic analysis of 100 randomly-selected *Armillaria* BUSCOs generated in this study, in conjunction with previously published *Armillaria* genomes, shows a strongly supported sister relationship with an *A. mellea* specimen from France (100% BS) (Fig. 8A). Phylogenetic analysis of all ITS sequences characterized as *A. mellea* from GenBank shows that this specimen is conspecific with specimens from eastern North American (Fig. 8B).

DISCUSSION

The formation of carpophoroids associated with species of *E. abortivum* have traditionally been thought to be the result of an *Armillaria* species attacking and parasitizing *Entoloma* sporocarps (11), a conclusion drawn based on the fact that *Armillaria* species are wide-spread forest pathogens (12). However, subsequent studies have shown the opposite: the production of carpophoroids are the result of *E. abortivum* disrupting the development of *Armillaria* sporocarps (14). Here, we employed RNA sequencing and differential gene expression analysis on field-collected fungal tissue of

each of the three components of this association to better understand the mechanistic basis of this interaction. We determined that *E. abortivum* reads in the metatranscriptome of the carpophoroid tissue—which can be interpreted as a measure of living tissue—are almost 35 times more abundant in the carpophoroid tissue compared to *A. mellea* reads (Fig. 6). This finding suggests that carpophoroids are structures that result from *E. abortivum* parasitizing, and eventually killing, its *Armillaria* host under natural conditions. Additionally, the genetic differences between carpophoroids and sporocarps is much smaller for *E. abortivum* than for *Armillaria* (Figs. 3, 4, and 7) , which could be suggestive that mycoparasitism is part of the life history of *E. abortivum* and fewer genetic shifts are necessary to transition between the carpophoroid and sporocarp.

Fungal-fungal necrotrophic mycoparasitic interactions are multistage processes that are best studied in model species, such as those in the genera *Trichoderma*, *Coniothyrium, Clonostachys* and *Tolypocladium* (17). Genomic and transcriptomic studies of necrotrophic mycoparasites show a convergence of significant genetic mechanisms at each stage (17). The *E. abortivum* genes that are upregulated with statistical significance in the carpophoroid tissue are largely consistent with other examples of necrotrophic mycoparasites in the Ascomycota. In the carpophoroid tissues we analyzed, *E. abortivum* appears to employ much of its energy on recognition and defense responses (Fig. 5). Inversely, the *Armillaria* sporocarps we analyzed illuminate possible mechanisms by which these two species recognize one another and how *Armillaria* responds to parasitism (Fig. 5).

The genetics of the* Entoloma-Armillaria *mycoparasitic interaction. A crucial step in a successful mycoparasite's life history is the ability to sense its host. Genes involved in the recognition of the fungal prey include those that code for GPCRs (15, 17). However, we did not find any of these genes that were differentially expressed by *E. abortivum* in the carpophoroid tissue (Fig. 3). Given the significantly fewer number of *Armillaria* reads in the carpophoroid tissue compared to *E. abortivum*, we presume that these carpophoroids are relatively advanced in age, and expression of the genes used for sensing the presence of the host are no longer necessary.

We also identified three *E. abortivum* genes that code for β-trefoil-type lectins—proteins that bind to galactose units of sugar chains (20)—that were significantly upregulated in the carpophoroid tissue (Figs. 3 and 5). In *Trichoderma* species, the recognition, attachment, and coiling around a fungal substrate is dependent on the recognition of lectins expressed by the fungal host (21, 22). Interestingly, the most abundant and differentially expressed gene produced in the *Armillaria* sporocarps, the substrate to which *E. abortivum* hyphae attach, codes for a cell wall galactomannoprotein (Figs. 4 and 5). These proteins belong to a group of polysaccharides which consist of a mannose backbone with galactose side chains, and are known to make up a major part of the cell wall of some fungal species (23). This particular galactomannoprotein appears to be specific to *Armillaria* species. Watling (11) commented on the highly specific nature of this interaction and that it has only been documented occurring between *E. abortivum* and *Armillaria* species. One possible mediator of the specificity of this interaction could be the galactose sugars on the mannose protein (only known thus far from *Armillaria* species) are the means by which

253 *E. abortivum* β-trefoil-type lectins recognize and attach to its *Armillaria* host. However,
254 more genome sequencing of other Agaricales species is needed to determine whether
255 this protein is truly specific to species in the genus *Armillaria*.

256 During mycoparasitic interactions, the fungal host responds by mounting its own
257 defense, and a successful mycoparasite must be able to cope with this counterattack
258 (15, 17). Two of the most abundant and significantly upregulated *E. abortivum* genes in
259 the carpophoroid tissue code for oxalate decarboxylases—enzymes responsible for the
260 degradation of oxalic acid (OA) (Figs. 3, 4, 5D, Table 1). In at least one known well-
261 studied mycoparasitic interaction, OA is secreted by the fungal host, *Sclerotinia*
262 *sclerotiorum*, in reaction to penetration by its mycoparasite, *Coniothyrium minitans*. The
263 acidic environment created by the secreted OA inhibits conidial germination and
264 suppresses mycelial growth of *C. minitans* (24). However, *C. minitans* nullifies the
265 growth-suppressing effects of OA or OA-mediated low pH by degrading the OA (25, 26),
266 an enzymatic process largely mediated by oxalate decarboxylase. Because of this,
267 oxalate decarboxylase plays an imperative role in mycoparasitism as OA degradation is
268 vital for infection of the fungal host (27).

269 The secretion of OA is also a broader defense mechanism employed by some
270 plant pathogens to compromise the defense responses of the host plant by creating an
271 acidic environment (28). One of the components of the plant-parasitic arsenal of
272 *Armillaria* species may be the production of OA (29). One differentially upregulated
273 gene in *Armillaria* sporocarps is isocitrate lyase (Fig. 5), which is involved with OA
274 biosynthesis in other fungal pathogens (30, 31). We have two hypotheses for the
275 upregulation of isocitrate lyase in the apparently asymptomatic *Armillaria* sporocarp

tissue. An explanation might be that isocitrate lyase is more upregulated in situations where *Armillaria* is in contact with a plant host and OA biosynthesis is high. One might also suggest that *Armillaria* is monitoring the close proximity of *E. abortivum* and it is preemptively launching a defense before hyphal contact is made. However, the upregulation of oxalate decarboxylases by *E. abortivum* suggests it has evolved a sophisticated strategy to inactivate the potentially lethal defenses of *Armillaria* exhibited by the subsequent downregulation of isocitrate lyase in the carpophoroid tissue (Fig. 5).

Other ways that mycoparasites cope with the counterattack launched by their host include actively extruding host-secreted toxins. Here, we hypothesize that active extrusion of toxins secreted by the host occurs in the *E. abortivum* carpophoroid tissue via membrane transporters in the ABC superfamily (32–34). Three ABC transporters were differentially expressed in the carpophoroid tissue (Fig. 3). Another group of genes that were differentially expressed by *E. abortivum* in the carpophoroid belong to the major facilitator superfamily (MFS) transporters (Fig. 3). In *C. rosea*, there was selection for genes in this family that were related to drug resistance, and the transport of secondary metabolites, small organic compounds and carbohydrates (35). Their importance to mycoparasitism in *C. rosea* is predicted to invoke efflux-mediated protection against exogenous or endogenous secondary metabolites and nutrient uptake (35). MFS transporters have also been shown to be induced in other mycoparasitic species (16, 36), but their exact biological roles have not been investigated.

In mycoparasitism, the final death of the host often results from the synergistic actions of cell wall-hydrolytic enzymes and antifungal secondary metabolites (15, 17).

No secondary metabolite gene clusters identified in the *E. abortivum* transcriptome were significantly upregulated in the carpophoroid tissue (Fig. 3). In some mycoparasitic relationships, the secretion of secondary metabolites occurs early on in the interaction, including in *E. weberi*, which secretes toxic compounds that kill the leafcutter ant garden before contact (5). In culture experiments between *Armillaria* isolates and *E. abortivum*, the growth of *Armillaria* was severely inhibited by the presence of *E. abortivum* (37). This suggests that *E. abortivum* may potentially secrete a toxic compound early in the interaction that inhibits the growth of *Armillaria*. Given that significantly more of the living tissue in the carpophoroids belonged to *E. abortivum* (Fig. 6), it is possible that much of the *Armillaria* tissue was killed preceding the full development of the carpophoroid.

We hypothesize that the upregulated β-trefoil-type lectin in *E. abortivum* that may be important in hyphal recognition may also be cytotoxic towards *Armillaria*. This type of lectin has sequence homology, as well as putative structural similarity, to the B-subunit of ricin, a toxic protein from the castor bean *Ricinus communis* (38). An array of β-trefoil-type lectins have been characterized from the sporocarps of the mushroom-forming species *Clitocybe nebularis* (39), *Coprinus cinerea* (40), *Macrolepiota procera* (41) and *Boletus edulis* (42). These mushroom lectins exhibit entomotoxic activity (43) as well as nematoxic activity (40, 41, 44). Taken together, it is possible that these *E. abortivum* β-trefoil-type lectins may also function as toxins towards *Armillaria*. While the *E. abortivum* genes coding for these lectins are not in the highest abundance in the carpophoroid tissue (Fig. 5), this could be because most of the *Armillaria* sporocarp tissue is already dead and the potential lethal effects of these genes are no longer necessary.

322 Chitin is an essential polymer in fungal cell walls (45) and is an important target
323 during mycoparasitic attack (17). Indicative of the importance of chitinases in
324 mycoparasitic interactions, members of the genus *Trichoderma*, as well as *T.*
325 *ophioglossoides* and *E. weberi,* have an increased number of genes coding for the
326 glycoside hydrolase family 18 (16, 46–49). Nine fungal chitinases were detected in the
327 transcriptome of *E. abortivum*, although only two were differentially expressed in the
328 carpophoroid tissue (Fig. 3) and were not abundant in comparison to other genes,
329 suggesting minimal significance at this stage in carpophoroid development. One
330 possibility for this difference in abundance could be the result of the putatively acidic pH
331 in the carpophoroid that we infer based on the high gene expression of oxalate
332 decarboxylases. In *C. minitans*, chitinase activity is positively correlated with ambient
333 pH ranging from three to eight (50), so it is possible that chitinase activity in *E.*
334 *abortivum* will increase after a neutral pH is restored.
335 Some of the putatively mycoparasitism-related genes outlined above were also
336 differentially expressed by *Armillaria* in the carpophoroid tissue. These include genes
337 that code for MFS, ABC transporters, chitinases, and secondary metabolite gene
338 clusters (Fig. 3). This suggests that *Armillaria* may be using many of the same genetic
339 mechanisms to defend itself against parasitism by *E. abortivum*. Additionally, the degree
340 of expression changes—both in the number of differentially expressed genes and the
341 log-fold change (logFC)—between the sporocarp and carpophoroid is much greater in
342 *Armillaria* compared to *E. abortivum* (Fig. 3, 4, 7), which could be a reflection of the
343 level of defense *Armillaria* is mounting. However, this defense is apparently not enough
344 to overcome the parasitic adaptations of *E. abortivum*.

***Gene and CAZyme content of* E. abortivum.** The number of predicted gene models in the transcriptome of *E. abortivum* was 9,728, which is markedly fewer than the number of gene models in the genomes of its closest sequenced relatives (Fig. 2B). Additionally, relative to other closely related mushroom species, *E. abortivum* also exhibits a strong reduction in several gene families encoding CAZymes (Fig. 2C), and contains no cellobiohydrolases, xylanases, or polysaccharide monooxygenases. This is similar to *E. weberi*, which also has a reduced genome and CAZyme repertoire—hypothesized to be the result of its highly specialized interaction with leafcutter ant gardens (46). Therefore, it is possible that *E. abortivum* only retained the CAZymes and accessory genes necessary to interact with *Armillaria* species. While a genome sequence of *E. abortivum* will be necessary to confirm this reduction, the BUSCO analysis verified that the *E. abortivum* transcriptome contains nearly 95% of the core set of eukaryotic genes.

Another possibility for the reduction in CAZymes could be explained by a broader nutritional strategy employed by *Entoloma* species, some of which form ectomycorrhiza-like structures on host plant species (51–53). Ectomycorrhizal species have a marked reduction in CAZymes in comparison to their saprotrophic ancestors (54), which we also observe with *Tricholoma matsutake* (Fig. 2C). However, microscopic analyses of *Entoloma* ectomycorrhizae-like structures suggest that some species destroy root meristems and young root cells, suggestive of a more parasitic relationship (51, 52). One explanation is that *Entoloma* species are actually parasites of true ectomycorrhizae. This explanation would also add credence to the evidence that *Entoloma* species are difficult to culture and are slow growing (53). Additional research

368 to understand the nutritional strategy employed by this lineage will inform us as to
369 whether fungal parasitism in this group is more common than it is currently understood
370 to be.
371
372 ***Identity of* Armillaria *species in this interaction.*** Phylogenomic analysis of the
373 *Armillaria* transcripts generated in this study suggest that the *Armillaria* species
374 parasitized in this particular relationship is sister to an *A. mellea* specimen collected
375 from western Europe (Fig. 8A). An ITS-based phylogenetic analysis shows the
376 *Armillaria* specimen collected in this study is conspecific with other *A. mellea* collections
377 from eastern North America (Fig. 8B). *Armillaria mellea* has previously been identified
378 as a host of *E. abortivum* (11, 14), but this interaction does not appear specific to just *A.*
379 *mellea*. Interestingly, *Armillaria* species parasitized by *E. abortivum* appear to be only
380 those present in Eastern North America and Asia (14, 37, 55).
381
382 ***Conclusions.*** Data from this study support the hypothesis that *E. abortivum* is a
383 mycoparasite of *Armillaria* sporocarps. Three β-trefoil-type lectins are differentially
384 expressed by *E. abortivum* in the carpophoroid tissue, and we propose that these
385 lectins mediate recognition with *Armillaria* sporocarps through binding to an *Armillaria*-
386 specific galactomannoprotein. Additionally, through the use of oxalate decarboxylase, *E.*
387 *abortivum* is likely defending against the secretion of OA by *Armillaria*. These strategies
388 employed by *E. abortivum* for recognition and defense are similar to mechanisms
389 utilized by other mycoparasites, suggesting that even distantly related mycoparasites
390 utilize similar genetic mechanisms to mediate mycoparasitic interactions. While we were

able to speculate about what is occurring during other stages of mycoparasitism (i.e. sensing the host and killing and consuming the host), future studies using both culture methods and metatranscriptomics of naturally collected carpophoroids at different life stages (i.e. younger and older specimens) will be necessary to completely tease apart the mycoparasitic strategies employed by *E. abortivum*.

MATERIALS AND METHODS

Sample collection, preparation, and sequencing. Sporocarps of *Armillaria* sp., *E. arbotivum*, and the mixed-tissue carpophoroids were observed fruiting in proximity to one another on 18 September 2015 within the Baker Woodlot and Rajendra Neotropical Migrant Bird Sanctuary, Michigan State University, East Lansing, MI 48823 (42°42'56.4" N, 84°28'34.4" W) (collection accession: JRH 2446). Entire sporocarps were collected and immediately flash frozen in liquid nitrogen and subsequently stored at -80°C. At the time of processing, three biological replicates of each of the three tissue types (*Armillaria sp*. sporocarp, *E. abortivum* sporocarp, and carpophoroid), were individually ground in liquid N_2. Total RNA was then extracted from the ground tissue using the Qiagen RNeasy kit (Qiagen Inc., Hilden, Germany) according to manufacturer's protocol. RNA concentration and quality for each of the samples were assessed on a DeNovix DS-11 FX Spectrophotometer (DeNovix Inc., Wilmington, DE 19810, USA) and then shipped directly to the University of Minnesota's Genomics Center (https://genomics.umn.edu). Three technical replicates were sequenced for each biological replicate. Transcriptomic and metatranscriptomic libraries were constructed with the TruSeq Standard Total RNA Library Preparation Kit with Ribo-Zero ribosomal

reduction following the protocol developed by Schuierer et al. (56). Nucleotide sequencing was performed on the Illumina HiSeq 2500 System (Illumina Inc., San Diego, USA) and paired-end RNA sequence reads of 51 bp were generated for further analysis.

De novo transcriptome assembly, transcript abundance estimation and gene expression analysis. The quality of the raw reads was assessed using FastQC version 0.11.9 (https://www.bioinformatics.babraham.ac.uk/projects/fastqc). The range of the number of reads for each condition are as follows: *E. abortivum* sporocarps ranged from 10,584,302 to 14,473,328; *Armillaria* sporocarps ranged from 11,712,320 to 12,431,979; and the carpophoroids ranged from 9,146,682 to 12,852,086. Sequencing adaptors were trimmed and contaminants filtered for each sample using bbduk (https://jgi.doe.gov/data-and-tools/bbtools/bb-tools-user-guide/bbduk-guide/). Prior to transcriptome assembly, *k-mer* hash sizes were estimated with *khmer* (57). De novo assemblies were constructed independently for both *Armillaria* sp. and *E. arbotivum* with Trinity version 2.11.0 (58) using the trimmed reads generated from the respective sporocarp reads. Assembly statistics for both transcriptomes were generated with QUAST version 5 (59) and transcriptome completeness was assessed by determining the percentage of sequenced BUSCOs in each (60).

The results of the *de novo* transcriptome assemblies were used as references to perform sample-specific expression analysis. The trimmed mushroom reads from each of the nine replicates were mapped against their respective reference transcriptomes using Bowtie2 (61) followed by calculation of abundance estimates using RSEM (62).

437 The trimmed carpophoroid reads were also subsequently mapped, following the same
438 protocol as described above, to both the *Armillaria* sp. and *E. arbotivum* transcriptomes.
439 Because of the close phylogenetic relatedness between these two species, and to filter
440 out poorly aligned reads, we only retained mapped reads for all samples that had a
441 MAPQ value of 30 and above, which is equivalent to reads that have a 99.9% chance of
442 hitting the correct match. The R package edgeR (63) and TMM normalization (64) were
443 used to determine differentially expressed transcripts between: 1) *Armillaria* sporocarps
444 and carpophoroids, and 2) *E. abortivum* sporocarps and carpophoroids. Genes were
445 considered differentially expressed if they had a logFC of two or greater and an FDR-
446 adjusted *p*-value, or *q*-value, of < 0.05. All statistical analyses for the packages listed
447 above were conducted using R version 4.0.3 (http://www.r-project.org/).
448 We used SAMtools (65) to determine the number of reads from the
449 carpophoroids that mapped to our reference transcriptomes of *E. abortivum* and our
450 particular *Armillaria* species. To understand whether the number of reads that mapped
451 to the carpophoroids differed significantly between each fungal species, we performed
452 an *F*-test of equality of variances, and then a two-tailed *t*-test assuming unequal
453 variance with a *p*-value < 0.05 denoting significance.
454
455 ***Sporocarp Transcriptome and Carpophoroid Metatranscriptome Annotation.*** We
456 annotated the *Armillaria* sp. and *E. abortivum* transcriptomes using Trinotate version 3.2
457 (66). Briefly, the transcripts were translated to coding protein sequences using
458 TransDecoder version 5.5.0 (http://transdecoder.github.io) following identification of the
459 longest open reading frames. To identify the most likely homologous sequence data, we

used *blastx* on the transcripts and *blastp* on the predicted protein sequences (67). Using the predicted protein sequences, we also ran a HMMER (68) search against the PFAM database (69) to identify conserved domains that might be suggestive of function. We also compared these results to currently curated annotation databases such as Gene Ontology (GO) (70) and Kyoto Encyclopedia of Genes and Genomes (KEGG) (71–73). Additionally, we used dbCAN2 (74) to annotate the CAZymes present in both species and compared their CAZy content to other closely related Agaricales species (19, 75–77). Finally, we used antiSMASH version 5.0 (78) to identify transcripts that belong to secondary metabolite gene clusters for both *Armillaria* and *E. abortivum*.

Phylogenetic analysis of* Armillaria *transcripts. In order to identify the specific species of *Armillaria* associated in this relationship, we identified BUSCOs (60) from the transcriptome of our *Armillaria* sporocarps along with other *Armillaria* and Physalacriaceae species with previously sequenced genomes (19; 79–81). We randomly selected 100 BUSCOs to reconstruct a phylogenomic tree from the six *Armillaria* specimens (19, 79), *Guyanagaster necrorhizus* (81) and *Cylindrobasidium torrendii* (80), which served as the outgroup. Protein-coding sequences were aligned using MAFFT version 7 (82) and non-informative sites and non-aligning regions were trimmed with Gblocks (83). The 100 BUSCOs were concatenated into a supermatrix with 64,436 sites. This supermatrix was used to infer a species tree and branch support using RAxML-NG (84), using a partitioned WAG+G model, where each data partition represented an individual BUSCO.

To supplement the small number of *Armillaria* species with sequenced genomes, we also extracted the internal transcribed spacer (ITS) region from our *Armillaria* transcriptome, including the regions 18S, ITS1, 5.8S, ITS2, and 28S, using ITSx (85). Given the close relationship of our *Armillaria* species to *A. mellea*, we pulled all *A. mellea* ITS sequences from GenBank that included associated location metadata (86–100) (Table S1). These sequences were aligned using MAFFT version 7 (82), with refinements to the alignment performed manually. RAxML-NG (84) was used to reconstruct this phylogeny. Taxa used to root this phylogeny included *A. gemina*, *A. sinapina*, *A. puiggarii* and *A. luteobubalina*—all members of the sister lineage to *A. mellea fide* (13).

Data and code availability. The raw reads generated during this study have been deposited in the NCBI Sequence Read Archive under the BioProject PRJNAXXXXX, while the assembled transcriptomes have been deposited in the NCBI Transcriptome Shotgun Assembly Sequencing Database under the records XXXXXXXXX and XXXXXXXX. All other associated data and code are available at https://github.com/HerrLab/Koch_Arm-Ento_2021.

Acknowledgements

We would like to give special thanks to Andrew Loyd and Eva Skific for providing photos and to Greg Bonito at Michigan State University and his trusty -80°C freezer for generously storing sporocarp and carpophoroid tissue until we were able to transport the tissue to our laboratory. We also want to thank the anonymous reviewers who

provided feedback and comments on the initial submission of this manuscript. This work was completed using the Holland Computing Center of the University of Nebraska, which receives support from the Nebraska Research Initiative. This research was directly supported by start-up funding from the University of Nebraska Agricultural Research Division and the University of Nebraska Office of Research and Economic Development. Additionally, JRH acknowledges funding from the US National Air & Space Administration (Grant #80NSSC17K0737), the US National Science Foundation (EPSCoR Grant #1557417), and US National Institute of Justice (Grant #2017-IJ-CX-0025), all of which indirectly supported this research through the support of research in his laboratory. All of the funding agencies had no role in study design, data collection and interpretation, or the decision to submit the work for publication.

Conflict of Interest Statement

On behalf of all authors, the corresponding author states that there is no conflict of interest.

Author Contributions

JRH initiated the work and sampled field collections; RAK extracted RNA from all the tissue samples and performed all the laboratory work; RAK and JRH performed the experiments, processed the experimental data, analyzed the data, designed the figures, and drafted the manuscript.

REFERENCES

1. Zeilinger S, Omann M. 2007. *Trichoderma* biocontrol: signal transduction pathways involved in host sensing and mycoparasitism. *Gene Regul Syst Bio* **1**:227–234.
2. Sun Z-B, Li S-D, Ren Q, Xu J-L, Lu X, Sun M-H. 2020. Biology and applications of *Clonostachys rosea*. *J Appl Microbiol* **129**:486–495.
3. Quandt CA, Kepler RM, Gams W, Araújo JPM, Ban S, Evans HC, Hughes D, Humber R, Hywel-Jones N, Li Z, Luangsa-Ard JJ, Rehner SA, Sanjuan T, Sato H, Shrestha B, Sung G-H, Yao Y-J, Zare R, Spatafora JW. 2014. Phylogenetic-based nomenclatural proposals for Ophiocordycipitaceae (Hypocreales) with new combinations in *Tolypocladium*. *IMA Fungus* **5**:121–134.
4. Currie CR, Mueller UG, Malloch D. 1999. The agricultural pathology of ant fungus gardens. *Proc Natl Acad Sci U S A* **96**:7998–8002.
5. Reynolds HT, Currie CR. 2004. Pathogenicity of *Escovopsis weberi*: the parasite of the attine ant-microbe symbiosis directly consumes the ant-cultivated fungus. *Mycologia* **96**:955–959.
6. Redhead SA, Ammirati JF, Walker GR, Norvell LL, Puccio MB. 1994. *Squamanita contortipes*, the Rosetta Stone of a mycoparasitic agaric genus. *Can J Bot* **72**:1814–1828.
7. Griffith GW, Piotr Gajda K, Detheridge AP, Douglas B, Bingham J, Turner A, Bowmaker V, Evans DA, McAdoo WG, Dentinger BTM. 2019. Strangler unmasked: Parasitism of *Cystoderma amianthinum* by *Squamanita paradoxa* and *S. pearsonii*. *Fungal Ecol* **39**:131–141.

8. Weber R, Webster J. 1996. *Volvariella surrecta*: An uncommon mycoparasite. *Mycologist* **10**:160.
9. Both EE. 2006. Personal encounters with the parasitic bolete. *Field Mycol* **7**:1–7.
10. Buller A. 1924. *Researches on Fungi.* Longmans, London, UK.
11. Watling R. 1974. Dimorphism in *Entoloma abortivum*. *Bull Soc Linn Lyon, Num Spec* **43**:449–470.
12. Baumgartner K, Coetzee MPA, Hoffmeister D. 2011. Secrets of the subterranean pathosystem of *Armillaria*. *Mol Plant Pathol* **12**:515–534.
13. Koch RA, Wilson AW, Séné O, Henkel TW, Aime MC. 2018. Resolved phylogeny and biogeography of the root pathogen *Armillaria* and its gasteroid relative, *Guyanagaster*. *BMC Evol Biol* **17**:33.
14. Lindner Czederpiltz DL, Volk TJ, Burdsall HH, Jr. 2001. Field observations and inoculation experiments to determine the nature of the carpophoroids associated with *Entoloma abortivum* and *Armillaria*. *Mycologia* **93**:841–851.
15. Druzhinina IS, Seidl-Seiboth V, Herrera-Estrella A, Horwitz BA, Kenerley CM, Monte E, Mukherjee PK, Zeilinger S, Grigoriev IV, Kubicek CP. 2011. Trichoderma: the genomics of opportunistic success. *Nat Rev Microbiol* **9**:749–759.
16. Quandt CA, Di Y, Elser J, Jaiswal P, Spatafora JW. 2016. Differential expression of genes involved in host recognition, attachment, and degradation in the mycoparasite Tolypocladium ophioglossoides. *G3* **6**:731–741.
17. Karlsson M, Atanasova L, Jensen DF, Zeilinger S. 2017. Necrotrophic mycoparasites and their genomes. *Microbiol Spectr* **5**:FUNK-0016-2016.

574 18. Ross-Davis AL, Stewart JE, Hanna JW, Kim MS, Knaus BJ, Cronn R, Rai H,
575 Richardson BA, McDonald GI, Klopfenstein NB. 2013. Transcriptome of an
576 *Armillaria* root disease pathogen reveals candidate genes involved in host
577 substrate utilization at the host–pathogen interface. *For Pathol* **43**:468–477.
578 19. Sipos G, Prasanna AN, Walter MC, O'Connor E, Bálint B, Krizsán K, Kiss B,
579 Hess J, Varga T, Slot J, Riley R, Bóka B, Rigling D, Barry K, Lee J, Mihaltcheva
580 S, LaButti K, Lipzen A, Waldron R, Moloney NM, Sperisen C, Kredics L,
581 Vágvölgyi C, Patrignani A, Fitzpatrick D, Nagy I, Doyle S, Anderson JB, Grigoriev
582 IV, Güldener U, Münsterkötter M, Nagy L. 2017. Genome expansion and lineage-
583 specific genetic innovations in the forest pathogenic fungi *Armillaria*. *Nat Ecol*
584 *Evol* **1**:1931–1941.
585 20. Dodd RB, Drickamer K. 2001. Lectin-like proteins in model organisms:
586 implications for evolution of carbohydrate-binding activity. *Glycobiology* **11**:71R–
587 79R.
588 21. Inbar J, Chet I. 1992. Biomimics of fungal cell-cell recognition by use of lectin-
589 coated nylon fibers. *J Bacteriol* **174**:1055–1059.
590 22. Inbar J, Chet I. 1996. The role of lectins in recognition and adhesion of the
591 mycoparasitic fungus *Trichoderma* spp. to its host. *Adv Exp Med Biol* **408**:229–
592 231.
593 23. Latgé JP, Kobayashi H, Debeaupuis JP, Diaquin M, Sarfati J, Wieruszeski JM,
594 Parra E, Bouchara JP, Fournet B. 1994. Chemical and immunological
595 characterization of the extracellular galactomannan of *Aspergillus fumigatus*.
596 *Infect Immun* **62**:5424–5433.

24. Wei SJ, Li GQ, Jiang DH, Wang DB. 2004. Effect of oxalic acid on spore germination and mycelial growth of the mycoparasite *Coniothyrium minitans*. *Acta Phytopathol Sin* **34**:199–203.

25. Ren L, Li GQ, Han YC, Jiang DH, Huang HC. 2007. Degradation of oxalic acid by *Coniothyrium minitans* and its effects on production and activity of β-1,3-glucanases of this mycoparasite. *Biol Control* **43**:1–11.

26. Ren L, Li GQ, Jiang DH. 2010. Characterization of some culture factors affecting oxalate degradation by the mycoparasite *Coniothyrium minitans*. *J Appl Microbiol* **108**:173–180.

27. Zeng L-M, Zhang J, Han Y-C, Yang L, Wu M-d, Jiang D-H, Chen W, Li G-Q. 2014. Degradation of oxalic acid by the mycoparasite *Coniothyrium minitans* plays an important role in interacting with *Sclerotinia sclerotiorum*. *Environ Microbiol* **16**:2591–2610.

28. Cessna SG, Sears VE, Dickman MB, Low PS. 2000. Oxalic acid, a pathogenicity factor for *Sclerotinia sclerotiorum*, suppresses the oxidative burst of the host plant. *Plant Cell* **12**:2191–2200.

29. Dumas MT, Boyonoski N, Jeng RS. 1989. Oxalic acid production by species of *Armillaria* in the boreal mixedwood forest. In: Proc. 7th International Conference on Root and Butt Rots. 9–16 Aug. 1988, Vernon and Victoria, British Columbia. Forestry Canada, Pacific Forestry Centre, Victoria, B.C. 680 p. 593–601.

30. Munir E, Jun Yoon J, Tokimatsu T, Hattori T, Shimada M. 2001. A physiological role for oxalic acid biosynthesis in the wood-rotting basidiomycete *Fomitopsis palustris*. *Proc Natl Acad Sci U S A* **98**:11126–11130.

620 31. Wang Y, Wang Y. 2020. Oxalic acid metabolism contributes to full virulence and
621 pycnidial development in the poplar canker fungus *Cytospora chrysosperma*.
622 *Phytopathology* **110**:1319–1325.
623 32. Dubey M, Jensen DF, Karlsson M. 2015. The ABC transporter ABCG29 is
624 involved in H_2O_2 tolerance and biocontrol traits in the fungus *Clonostachys rosea*.
625 *Mol Genet Genom* **291**:677–686.
626 33. Ruocco M, Lanzuise S, Vinale F, Marra R, Turrà, Lois Woo S, Lorito M. 2009.
627 Identification of a new biocontrol gene in *Trichoderma* atroviride: the role of an
628 ABC transporter membrane pump in the interaction with different plant-
629 pathogenic fungi. *Mol Plant Microbe In* **22**:291–301.
630 34. Zhao H, Zhou T, Xie J, Cheng J, Chen T, Jiang D, Fu Y. 2020. Mycoparasitism
631 illuminated by genome and transcriptome sequencing of *Coniothyrium minitans*,
632 an important biocontrol fungus of the plant pathogen *Sclerotinia sclerotiorum*.
633 *Microb Genom* **6**:e000345.
634 35. Nygren K, Dubey M, Zapparata A, Iqbal M, Tzelepis GD, Brandström Durling M,
635 Funck Jensen D, Karlsson M. 2018. The mycoparasitic fungus *Clonostachys*
636 *rosea* responds with both common and specific gene expression during
637 interspecific interactions with fungal prey. *Evol Appl* **11**:931–949.
638 36. Atanasova L, Le Crom S, Gruber S, Coulpier F, Seidl-Seiboth V, Kubick CP,
639 Druzhinina IS. 2013. Comparative transcriptomics reveals different strategies of
640 *Trichoderma* mycoparasitism. *BMC Genom* **14**:121.
641 37. Cha JY, Igarashi T. 1996. Biological species of *Armillaria* and their mycoparasitic
642 associations with *Rhodophyllus abortivus* in Hokkaido. *Mycoscience* **37**:25–30.

643 38. Tregear JW, Roberts LM. 1992. The lectin gene family of *Ricinus communis*:
644 Cloning of a functional ricin gene and three lectin pseudogenes. *Plant Mol Biol*
645 **18**:515–525.
646 39. Pohleven J, Obermajer N, Sabotič J, Anžlovar S, Sepčić K, Kos J, Kralj B,
647 Štrukelj B, Brzin J. 2009. Purification, characterization and cloning of a ricin B-
648 like lectin from mushroom *Clitocybe nebularis* with antiproliferative activity
649 against human leukemic T cells. *Biochim Biophys Acta Gen Subj* **1790**:173–181.
650 40. Schubert M, Bleuler-Martinez S, Butschi A, Wälti MA, Egloff P, Stutz K, Yan S,
651 Wilson IBH, Hengartner MO, Aebi M, Allain FHT, Künzler M. 2012. Plasticity of
652 the β-trefoil protein fold in the recognition and control of invertebrate predators
653 and parasites by a fungal defence system. *PLoS Pathog* **8**:e1002706.
654 41. Žurga S, Pohleven J, Renko M, Bleuler-Martínez S, Sosnowski P, Turk D,
655 Künzler M, Kos J, Sabotič J. 2014. A novel beta-trefoil lectin from the parasol
656 mushroom (*Macrolepiota procera*) is nematotoxic. *FEBS J* **281**:3489–3506.
657 42. Bovi M, Cenci L, Perduca M, Capaldi S, Carrizo ME, Civiero L, Chiarelli LR,
658 Galliano M, Monaco HL. 2013. BEL beta-trefoil: a novel lectin with antineoplastic
659 properties in king bolete (*Boletus edulis*) mushrooms. *Glycobiology* **23**:578–592.
660 43. Sabotič J, Ohm RA, Künzler M. 2016. Entomotoxic and nematotoxic lectins and
661 protease inhibitors from fungal fruiting bodies. *Appl Microbiol Biotechnol* **100**:91–
662 111.
663 44. Pohleven J, Renko M, Magister S, Smith DF, Künzler M, Strukelj B, Turk D, Kos
664 J, Sabotič J. 2012. Bivalent carbohydrate binding is required for biological activity
665 of *Clitocybe nebularis* lectin (CNL), the N, N'-diacetyllactosediamine

(GalNAcbeta1-4GlcNAc, LacdiNAc)-specific lectin from basidiomycete *C. nebularis*. *J Biol Chem* **287**:10602–10612.

45. Latgé JP. 2007. The cell wall: a carbohydrate armour for the fungal cell. *Mol Microbiol* **66**:279–290.

46. de Man TJ, Stajich JE, Kubicek CP, Teiling C, Chenthamara K, Atanasova L, Druzhinina IS, Levenkova N, Birnbaum SS, Barribeau SM, Bozick BA, Suen G, Currie CR, Gerardo NM. 2016. Small genome of the fungus *Escovopsis weberi*, a specialized disease agent of ant agriculture. *Proc Natl Acad Sci U S A* **113**:3567–3572.

47. Kubicek CP, Herrera-Estrella A, Seidl-Seiboth V, Martinez DA, Druzhinina IS, Thon M, Zeilinger S, Casas-Flores S, Horwitz BA, Mukherjee PK, Mukherjee M, Kredics L, Alcaraz LD, Aerts A, Antal Z, Atanasova L, Cervantes-Badillo MG, Challacombe J, Chertkov O, McCluskey K, Coulpier F, Deshpande N, von Döhren H, Ebbole DJ, Esquivel-Naranjo EU, Fekete E, Flipphi M, Glaser F, Gómez-Rodríguez EY. Gruber S, Han C, Henrissat B, Hermosa R, Hernández-Oñate M, Karaffa L, Kosti I, Le Crom S, Lindquist E, Lucas S, Lübeck M, Lübeck PS, Margeot A, Metz B, Misra M, Nevalainen H, Omann M, Packer N, Perrone G, Uresti-Rivera EE, Salamov A, Schmoll M, Seiboth B, Shapiro H, Sukno S, Tamayo-Ramos JA, Tisch D, Wiest A, Wilkinson HH, Zhang M, Coutinho PM, Kenerley CM, Monte E, Baker SE, Grigoriev IV. 2011. Comparative genome sequence analysis underscores mycoparasitism as the ancestral life style of *Trichoderma*. *Genome Biol* **12**:R40.

688 48. Ihrmark K, Asmail N, Ubhayasekera W, Melin P, Stenlid J, Karlsson M. 2010.
689 Comparative molecular evolution of *Trichoderma* chitinases in response to
690 mycoparasitic interactions. *Evol Bioinform* **6**:1–26.
691 49. Xie BB, Qin QL, Shi M, Chen LL, Shu YL, Luo Y, Wang XW, Rong JC, Gong ZT,
692 Li D, Sun CY, Liu GM, Dong XW, Pang XH, Huang F, Liu W, Chen XL, Zhou BC,
693 Zhang YZ, Song ZY. 2014. Comparative genomics provides insights into
694 evolution of *Trichoderma* nutrition style. *Genome Biol Evol* **6**:379–390.
695 50. Han Y-C, Li G-Q, Yang L, Jiang D-H. 2011. Molecular cloning, characterization
696 and expression analysis of a *pacC* homolog in the mycoparasite *Coniothyrium*
697 *minitans. World J Microbiol Biotechnol* **27**:381–391.
698 51. Agerer R, Waller K. 1993. Mycorrhizae of *Entoloma saepium*: parasitism or
699 symbiosis? *Mycorrhiza* **3**:145–154.
700 52. Kobayashi H, Hatano K. 2001. A morphological study of the mycorrhiza of
701 *Entoloma clypeatum* f. *hybridum* on *Rosa multiflora*. *Mycoscience* **42**:83–90.
702 53. Shishikura M, Takemura Y, Sotome K, Maekawa N, Nakagiri A, Endo N. 2021.
703 Four mycelial strains of *Entoloma clypeatum* species complex form
704 ectomycorrhiza-like roots with *Pyrus betulifolia* seedlings in vitro, and one
705 develops fruiting bodies 2 months after inoculation. *Mycorrhiza* **31**:31–42.
706 54. Kohler A, Kuo A, Nagy LG, Morin E, Barry KW, Buscot F, Canbäck B, Choi C,
707 Cichocki N, Clum A, Colpaert J, Copeland A, Costa MD, Doré J, Floudas D, Gay
708 G, Girlanda M, Henrissat B, Herrmann S, Hess J, Högberg N, Johansson T,
709 Khouja H-R, LaButti K, Lahrmann U, Levasseur A, Lindquist EA, Lipzen A,
710 Marmeisse R, Martino E, Murat C, Ngan CY, Nehls U, Plett JM, Pringle A, Ohm

RA, Perotto S, Peter M, Riley R, Rineau F, Ruytinx J, Salamov A, Shah F, Sun H, Tarkka M, Tritt A, Veneault-Fourrey C, Zuccaro A, Mycorrhizal Genomics Initiative Consortium, Tunlid A, Grigoriev IV, Hibbett DS, Martin F. 2015. Convergent losses of decay mechanisms and rapid turnover of symbiosis genes in mycorrhizal mutualists. *Nat Genet* **47**:410–415.

55. Fukuda M, Nakashima E, Hayashi K, Nagasawa E. 2003. Identification of the biological species of *Armillaria* associated with *Wynnea* and *Entoloma abortivum* using PCR-RFLP analysis of the intergenic region (IGR) of ribosomal DNA. *Mycol Res* **107**:1435–1441.

56. Schuierer S, Carbone W, Knehr J, Petitjean V, Fernandez A, Sultan M, Roma G. 2017. A comprehensive assessment of RNA-seq protocols for degraded and low-quantity samples. *BMC Genom* **18**:1–13.

57. Crusoe MR, Alameldin HF, Awad S, Boucher E, Caldwell A, Cartwright R, Charbonneau A, Constantinides B, Edvenson G, Fay S, Fenton J, Fenzl T, Fish J, Garcia-Gutierrez L, Garland P, Gluck J, González I, Guermond S, Guo J, Gupta A, Herr JR, Howe A, Hyer A, Härpfer A, Irber L, Kidd R, Lin D, Lippi J, Mansour T, McA'Nulty P, McDonald E, Mizzi J, Murray KD, Nahum JR, Nanlohy K, Nederbragt AJ, Ortiz-Zuazaga H, Ory J, Pell J, Pepe-Ranney C, Russ ZN, Schwarz E, Scott C, Seaman J, Sievert S, Simpson J, Skennerton CT, Spencer J, Srinivasan R, Standage D, Stapleton JA, Steinman SR, Stein J, Taylor B, Trimble W, Wiencko HL, Wright M, Wyss B, Zhang Q, zyme e, Brown CT. 2015. The khmer software package: enabling efficient nucleotide sequence analysis. *F1000Res* **4**:900.

58. Grabherr MG, Haas BJ, Yassour M, Levin JZ, Thompson DA, Amit I, Adiconis X, Fan L, Raychowdhury R, Zeng Q, Chen Z, Mauceli E, Hacohen N, Gnirke A, Rhind N, di Palma F, Birren BW, Nusbaum C, Lindblad-Toh K, Friedman N, Regev A. 2011. Trinity: reconstructing a full-length transcriptome without a genome from RNA-Seq data. *Nat Biotechnol* **29**:644–652.

59. Mikheenko A, Prjibelski A, Saveliev V, Antipov D, Gurevich A. 2018. Versatile genome assembly evaluation with QUAST-LG. *Bioinformatics* **34**:i142–i150.

60. Seppey M, Manni M, Zdobnov EM. 2019. BUSCO: Assessing genome assembly and annotation completeness. In: Kollmar M (eds) Gene Prediction. Methods in Molecular Biology, vol 1962. Humana, New York, NW.

61. Langmead B, Salzberg SL. 2012. Fast gapped-read alignment with Bowtie 2. *Nat Methods* **9**:357–359.

62. Li B, Dewey CN. 2011. RSEM: accurate transcript quantification from RNA-Seq data with or without a reference genome. *BMC Bioinform* **12**:323.

63. Robinson MD, McCarthy DJ, Smyth GK. 2010. edgeR: a Bioconductor package for differential expression analysis of digital gene expression data. *Bioinformatics* **26**:139–140.

64. Robinson MD, Oshlack A. 2010. A scaling normalization method for differential expression analysis of RNA-seq data. *Genome Biol* **11**:R25.

65. Li H, Handsaker B, Wysoker A, Fennell T, Ruan J, Homer N, Marth G, Abecasis G, Durbin R, 1000 Genome Project Data Processing Subgroup. 2009. The Sequence Alignment/Map format and SAMtools. *Bioinformatics* **25**:2078–2079.

66. Bryant DM, Johnson K, DiTommaso T, Tickle T, Brian Couger M, Payzin-Dogru D, Lee TJ, Leigh ND, Kuo T-H, Davis FG, Bateman J, Bryant S, Guzikowski AR, Tsai SL, Coyne S, Ye WW, Freeman RM, Jr, Peshkin L, Tabin CJ, Regev A, Haas BJ, Whited JL. 2017. A tissue-mapped axolotl de novo transcriptome enables identification of limb regeneration factors. *Cell Rep* **18**:P762–P776.
67. Camacho C, Coulouris G, Avagyan V, Ma N, Papadopoulos J, Bealer K, Madden TL. 2009. BLAST+: architecture and application. *BMC Bioinform* **10**:421.
68. Wheeler TJ, Eddy SR. 2013. nhmmer: DNA homology search with profile HMMs. *Bioinformatics* **29**:3487–3489.
69. Finn RD, Bateman A, Clements J, Coggill P, Eberhardt RY, Eddy SR, Heger A, Hetherington K, Holm L, Mistry J, Sonnhammer ELL, Tate J, Punta M. 2014. Pfam: the protein families database. *Nucleic Acids Res* **42**:D222–D230.
70. Ashburner M, Ball CA, Blake JA, Botstein D, Butler H, Cherry JM, Davis AP, Dolinski K, Dwight SS, Eppig JT, Harris MA, Hill DP, Issel-Tarver L, Kasarskis A, Lewis S, Matese JC, Richardson JE, Ringwald M, Rubin GM, Sherlock G. 2000. Gene Ontology: tool for the unification of biology. *Nat Genet* **25**:25–29.
71. Kanehisa M, Goto S. 2000. KEGG: Kyoto Encyclopedia of Genes and Genomes. *Nucleic Acids Res* **28**:27–30.
72. Kanehisa M. 2019. Toward understanding the origin and evolution of cellular organisms. *Protein Sci* **28**:1947–1951.
73. Kanehisa M, Furumichi M, Sato Y, Ishiguro-Watanabe M, Tanabe M. 2021. KEGG: integrating viruses and cellular organisms. *Nucleic Acids Res* **49**:D545–D551.

779 74. Zhang H, Yohe T, Huang L, Entwistle S, Wu P, Yang Z, Busk PK, Xu Y, Yin Y.
780 2018. dbCAN2: a meta server for automated carbohydrate-active enzyme
781 annotation. *Nucleic Acids Res* **46**:W95–W101.
782 75. Miyauchi S, Kiss E, Kuo A, Drula E, Kohler A, Sánchez-García M, Morin E,
783 Andreopoulos B, Barry KW, Bonito G, Buée M, Carver A, Chen C, Cichocki N,
784 Clum A, Culley D, Crous PW, Fauchery L, Girlanda M, Hayes RD, Kéri Z, LaButti
785 K, Lipzen A, Lombard V, Magnuson J, Maillard F, Murat C, Nolan M, Ohm RA,
786 Pangilinan J, Pereira MF, Perotto S, Peter M, Pfister S, Riley R, Sitrit Y, Stielow
787 JB, Szöllősi G, Žifčáková L, Štursová M, Spatafora JW, Tedersoo L, Vaario LM,
788 Yamada A, Yan M, Wang P, Xu J, Bruns T, Baldrian P, Vilgalys R, Dunand C,
789 Henrissat B, Grigoriev IV, Hibbett D, Nagy LG, Martin FM. 2020. Large-scale
790 genome sequencing of mycorrhizal fungi provides insights into the early evolution
791 of symbiotic traits. *Nat Commun* **11**:5125.
792 76. Steindorff AS, Carver A, Calhoun S, Stillman K, Liu H, Lipzen A, He G, Yan M,
793 Pangilinan J, LaButti K, Ng V, Bruns TD, Grigoriev IV. 2020. Comparative
794 genomics of pyrophilous fungi reveals a link between fire events and
795 developmental genes. *Environ Microbiol* **23**:99–109.
796 77. Ruiz-Dueñas FJ, Barrasa JM, Sánchez-García M, Camarero S, Miyauchi S,
797 Serrano A, Linde D, Babiker R, Drula E, Ayuso-Fernández I, Pacheco R, Padilla
798 G, Ferreira P, Barriuso J, Kellner H, Castanera R, Alfaro M, Ramirez L, Pisabarro
799 AG, Riley R, Kuo A, Andreopoulos W, LaButti K, Pangilinan J, Tritt A, Lipzen A,
800 He G, Yan M, Ng V, Grigoriev IV, Cullen D, Martin F, Rosso MN, Henrissat B,
801 Hibbett D, Martínez AT. 2020. Genomic analysis enlightens Agaricales lifestyle

802 evolution and increasing peroxidase diversity. *Mol Biol Evol*
803 doi:10.1093/molbev/msaa301.
804 78. Blin K, Shaw S, Steinke K, Villebro R, Ziemert N, Yup Lee S, Medema MH,
805 Weber T. 2019. antiSMASH 5.0: updates to the secondary metabolite genome
806 mining pipeline. *Nucleic Acids Res* **47**:W81–W87.
807 79. Collins C, Keane TM, Turner DJ, O'Keeffe G, Fitzpatrick DA, Doyle S. 2013.
808 Genomic and proteomic dissection of the ubiquitous plant pathogen, *Armillaria*
809 *mellea*: Toward a new infection model system. *J Proteome Res* **12**:2552–2570.
810 80. Floudas D, Held BW, Riley R, Nagy LG, Koehler G, Ransdell AS, Younus H,
811 Chow J, Chiniquy J, Lipzen A, Tritt A, Sun H, Haridas S, LaButtie K, Ohm RA,
812 Kües U, Blanchette RA, Grigoriev IV, Minto RE, Hibbett DS. 2015. Evolution of
813 novel wood decay mechanisms in Agaricales revealed by the genome
814 sequences of *Fistulina hepatica* and *Cylindrobasidium torrendii*. *Fungal Genet*
815 *Biol* **76**:78–92.
816 81. Koch RA, Yoon GM, Arayal UK, Lail K, Amirebrahimi M, LaButti K, Lipzen A,
817 Riley R, Barry K, Henrissat B, Grigoriev IV, Herr JR, Aime MC. Symbiotic
818 nitrogen fixation in the reproductive structures of a basidiomycete fungus. *Curr*
819 *Biol*, Accepted.
820 82. Katoh K, Standley DM. 2013. MAFFT multiple sequence alignment software
821 version 7: improvements in performance and usability. *Mol Biol Evol* **30**:772–780.
822 83. Castresana J. 2000. Selection of conserved blocks from multiple alignments for
823 their use in phylogenetic analysis. *Mol Biol Evol* **17**:540–552.

824 84. Kozlov AM, Darriba D, Flouri T, Morel B, Stamatakis A. 2019. RAxML-NG: a fast,
825 scalable and user-friendly tool for maximum likelihood phylogenetic inference.
826 *Bioinformatics* **35**:4453–4455.
827 85. Bengtsson-Palme J, Ryberg M, Hartmann M, Branco S, Wang Z, Godhe A, De
828 Wit P, Sánchez-García M, Ebersberger I, de Sousa F, Amend A, Jumpponen A,
829 Unterseher M, Kristiansson E, Abarenkov K, Bertrand YJK, Sanli K, Eriksson KM,
830 Vik U, Veldre V, Nilsson RH. 2013. Improved software detection and extraction of
831 ITS1 and ITS2 from ribosomal ITS sequences of fungi and other eukaryotes for
832 analysis of environmental sequencing data. *Methods Ecol Evol* **4**:914–919.
833 86. Guo T, Wang HC, Xue WQ, Zhao J, Yang ZL. 2016. Phylogenetic analyses of
834 *Armillaria* reveal at least 15 phylogenetic lineages in China, seven of which are
835 associated with cultivated *Gastrodia elata*. *PLoS One* **11**:e0154794.
836 87. Coetzee MPA, Wingfield BD, Harrington TC, Dalevi D, Coutinho TA, Wingfield
837 MJ. 2000. Geographical diversity of *Armillaria mellea* s. s. based on phylogenetic
838 analysis. *Mycologia* **92**:105–113.
839 88. Coetzee MPA, Wingfield BD, Bloomer P, Wingfield MJ. 2005. Phylogenetic
840 analyses of DNA sequences reveal species partitions amongst isolates of
841 *Armillaria* from Africa. *Mycol Res* **109**:1223–1234.
842 89. Schneider-Maunoury L, Deveau A, Moreno M, Todesco F, Belmondo S, Murat C,
843 Courty P-E, Jąkalski M, Selosse M-A. 2020. Two ectomycorrhizal truffles, *Tuber*
844 *melanosporum* and *T. aestivum*, endophytically colonise roots of non-
845 ectomycorrhizal plants in natural environments. *New Phytol* **225**:2542–2556.

90. Coetzee MPA, Bloomer P, Wingfield MJ, Wingfield BD. 2011. Paleogene radiation of a plant pathogenic mushroom. *PLoS One* **6**:e28545.

91. Osmundson TW, Robert VA, Schoch CL, Baker LJ, Smith A, Robich G, Mizzan L, Garbelotto MM. 2013. Filling gaps in biodiversity knowledge for macrofungi: contributions and assessment of an herbarium collection DNA barcode sequencing project. *PLoS One* **8**:e62419.

92. Kasper-Pakosz R, Pietras M, Łuczaj Ł. 2016. Wild and native plants and mushrooms sold in the open-air markets of south-eastern Poland. *J Ethnobiol Ethnomed* **12**:45.

93. Hughes KW, Petersen RH, Lodge DJ, Bergemann SE, Baumgartner K, Tulloss RE, Lickey E, Cifuentes J. 2013. Evolutionary consequences of putative intra- and interspecific hybridization in agaric fungi. *Mycologia* **105**:1577–1594.

94. Potyralska A, Schmidt O, Moreth U, Łakomy P, Siwecki R. 2002. rDNA-ITS sequence of *Armillaria* species and a specific primer for *A. mellea*. *For Genet* **9**:119–124.

95. Ortega A, Moreno G, Platas G, Pelaez F. 2008. A new *Armillaria mellea* variant from tops of coastal sand dunes in southern Spain. *Mycotaxon* **104**:349–364.

96. Vu D, Groenewald M, de Vries M, Gehrmann T, Stielow B, Eberhardt U, Al-Hatmi A, Groenewald JZ, Cardinali G, Houbraken J, Boekhout T, Crous PW, Robert V, Verkley GJM. 2019. Large-scale generation and analysis of filamentous fungal DNA barcodes boosts coverage for kingdom fungi and reveals thresholds for fungal species and higher taxon delimitation. *Stud Mycol* **92**:135–154.

97. Binder M, Hibbett DS, Wang Z, Farnham WF. 2006. Evolutionary relationships of *Mycaureola dilseae* (Agaricales), a basidiomycete pathogen of a subtidal rhodophyte. *Am J Bot* **93**:547–556.

98. Haelewaters D, Dirks AC, Kappler LA, Mitchell JK, Quijada L, Vandegrift R, Buyck B, Pfister DH. 2018. A preliminary checklist of fungi at the Boston Harbor Islands. *Northeast Nat* **25**:45–76.

99. Kim M-S, Klopfenstein NB, Hanna JW, McDonald GI. 2006. Characterization of North American *Armillaria* species: genetic relationships determined by ribosomal DNA sequences and AFLP markers. *For Path* **36**:145–164.

100. Schnabel G, Ash JS, Bryson PK. 2005. Identification and characterization of *Armillaria tabescens* from the southeastern United States. *Mycol Res* **109**:1208–1222.

TABLE 1 Ten most highly expressed *E. abortivum* genes in sporocarps and carpophoroids

Gene	Annotation	Cond.	C (TMM)	S (TMM)	logFC	*q*-value
ENT_DN2762_c0_g3	Oxalate decarboxylase	C	68,724	238	-8.5	4.5×10^{-317}
ENT_DN1212_c0_g1	Hypothetical protein	C/S	55,939	12,590	-2.5	4.3×10^{-49}
ENT_DN3063_c0_g2	Oxalate decarboxylase	C	48,157	135	-8.8	0
ENT_DN1952_c0_g2	Acid phosphatase	C	19,999	677	-5.2	1.3×10^{-169}
ENT_DN4045_c1_g1	Hypothetical protein	C	19,965	3,374	-2.9	3.4×10^{-63}
ENT_DN5742_c0_g1	Hypothetical protein	C	11,229	23	-9.3	6.9×10^{-220}
ENT_DN4332_c0_g1	Hypothetical protein	C	11,038	607	-4.5	4.7×10^{-77}
ENT_DN1952_c0_g1	Acid phosphatase	C	10,766	673	-4.4	1.9×10^{-122}
ENT_DN2936_c0_g2	Hypothetical protein	C	9,212	3,686	NS	
ENT_DN3086_c0_g1	Hypothetical protein	C	9,076	1,563	-2.9	2.2×10^{-62}
ENT_DN1375_c0_g1	Trehalase	S	1,934	17,890	2.9	6.5×10^{-37}
ENT_DN5247_c0_g3	Hypothetical protein	S	2,718	7,204	NS	
ENT_DN761_c0_g2	Hypothetical protein	S	7,405	6,918	NS	
ENT_DN521_c0_g2	Hypothetical protein	S	6,045	6,424	NS	
ENT_DN852_c0_g1	Hypothetical protein	S	123	5,429	5.1	2.0×10^{-142}
ENT_DN3621_c0_g2	RNA polymerase	S	1,977	5,138	NS	
ENT_DN6707_c0_g1	Hypothetical protein	S	1,654	5,027	NS	
ENT_DN2379_c0_g1	TPR-like protein	S	4,862	5,017	NS	
ENT_DN466_c0_g1	Auxin efflux carrier	S	1,205	4,333	NS	

Cond.: condition in which each gene was most highly expressed, referring to either the carpophoroids (C) or sporocarps (S). NS: not significantly differentially expressed in either condition. Negative logFC values are significantly differentially upregulated in the carpophoroid, whereas positive values are significantly differentially upregulated in the sporocarp. Transcripts discussed in the text include two oxalate decarboxylases (ENT_DN2762_c0_g3, ENT_DN3063_c0_g2), three β-trefoil-type lectins (ENT_DN4359_c0_g1, ENT_DN1877_c0_g1, ENT_DN4255_c0_g1), three ABC transporters (ENT_DN1537_c0_g1, ENT_DN189_c0_g1, ENT_DN3860_c0_G1), two chitinases (ENT_DN2096_c0_g1, ENG_DN4507_c0_g3) and 14 MFS transcripts (ENT_DN409_c0_g1, ENT_DN1954_c0_g1, ENT_DN1998_c0_g1, ENT_DN2070_c0_g1, ENT_DN2744_c0_g1, ENT_DN3292_c0_g1, ENT_DN3474_c0_g1, ENT_DN3861_c0_g1, ENT_DN3943_c0_g1, ENT_DN3943_c0_g2, ENT_DN3981_c0_g1, ENT_DN4751_c0_g2, ENT_DN6588_c0_g1, ENT_DN6695_c0_g1).

TABLE 2 Ten most highly expressed *Armillaria* genes in sporocarps and carpophoroids

Gene	Annotation	Cond.	C (TMM)	S (TMM)	logFC	*q*-value
ARM_DN1755_c2_g1	Cell wall galactomannoprotein	S	0	36,479	13.5	4.0×10^{-182}
ARM_DN3840_c0_g1	Serine carboxypeptidase	S	12	29,472	6.7	7.9×10^{-100}
ARM_DN22943_c1_g1	Rab geranylgeranyltransferase	S	21	18,649	5.1	3.8×10^{-89}
ARM_DN1737_c0_g1	LysM-domain-containing protein	S	0	14,557	15.9	3.0×10^{-159}
ARM_DN1699_c3_g1	Hypothetical protein	S	9	12,848	5.8	1.6×10^{-94}
ARM_DN1314_c0_g1	Chondroitin AC/alginate lyase	S	102	11,436	2.2	3.7×10^{-25}
ARM_DN20980_c0_g1	Glycopeptide	S	0	10,449	15.4	3.4×10^{-139}
ARM_DN8135_c0_g1	Rasp f 7 allergen	S	0	9,014	11.5	1.8×10^{-58}
ARM_DN4971_c0_g2	Aldehyde dehydrogenase	S	103	8,688	NS	
ARM_DN1205_c0_g1	Hypothetical protein	S/C	9,049	8,348	-4.8	2.1×10^{-74}
ARM_DN5170_c0_g1	Hypothetical protein	C	2,086	377	-7.1	6.9×10^{-150}
ARM_DN23207_c0_g2	Senescence-associated	C	1,711	2,482	-4.1	6.6×10^{-61}
ARM_DN996_c0_g1	Senescence-associated	C	1,423	1,090	-5.0	3.0×10^{-73}
ARM_DN409_c1_g1	Elongation factor 1-alpha	C	769	1,154	-4.1	4.0×10^{-155}
ARM_DN1893_c0_g1	Hypothetical protein	C	722	58	-8.3	5.3×10^{-109}
ARM_DN693_c0_g1	Hypothetical protein	C	520	840	-3.9	1.1×10^{-48}
ARM_DN1222_c0_g1	CYS3-cystathionine gamma-lyase	C	485	717	-4.1	5.5×10^{-27}
ARM_DN1146_c0_g4	Heat shock protein 70	C	431	2,361	-2.2	1.7×10^{-54}
ARM_DN3800_c0_g1	ATP synthase F1	C	300	4,686	NS	

Cond.: condition in which each gene was most highly expressed, referring to either the carpophoroids (C) or sporocarps (S). NS: not significantly differentially expressed in either condition. Negative logFC values are significantly differentially upregulated in the carpophoroid, whereas positive values are significantly differentially upregulated in the sporocarp. Transcripts discussed in the text were an isocitrate lyase (ARM_DN1_c7_g1), two putative senescence-associated proteins (ARM_DN23207_c0_g2, ARM_DN996_c0_g1), and a heat shock protein (ARM_DN1146_c0_g4).

947

948 **FIG 1** The components of this fungal interaction in nature. (A) *Armillaria* sporocarps. (B)
949 *Entoloma abortivum* sporocarps; photo taken by Eva Skific. (C) Carpophoroids. (D) A
950 group of *E. abortivum* sporocarps and carpophoroids, with the carpophoroids indicated
951 by arrows; photo taken by Andrew Loyd. Scale bars in A–C are equal to 1 cm and in D
952 are equal to 10 cm.

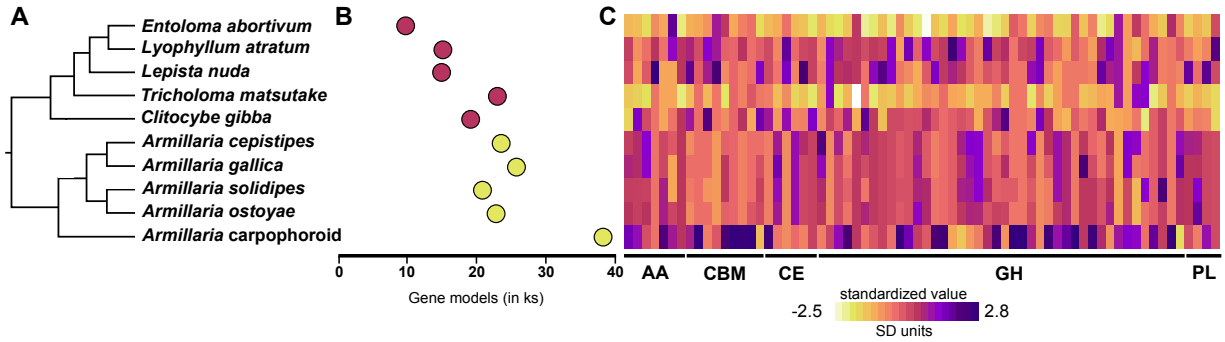

953

954 **FIG 2** Number of total gene models and gene copy numbers of CAZymes. (A) A
955 representative phylogeny is a representation based off phylogenetic evidence from
956 Sipos et al. (2017) and Dentinger et al. (2016). (B) Number of gene models in the
957 transcriptome of the *Armillaria* and *E. abortivum* generated in this study, along with
958 those of closely related species from previously generated genomic data. (C) Heat map
959 showing gene copy numbers of plant cell wall degrading enzymes detected in the
960 transcriptomes of *E. abortivum* and *Armillaria*, along with other closely related species.
961 Abbreviations: AA: Auxiliary Activities; CBM: Carbohydrate-Binding Modules; CE:
962 Carbohydrate Esterase; GH: Glycoside Hydrolase; PL: Polysaccharide Lyase.

963

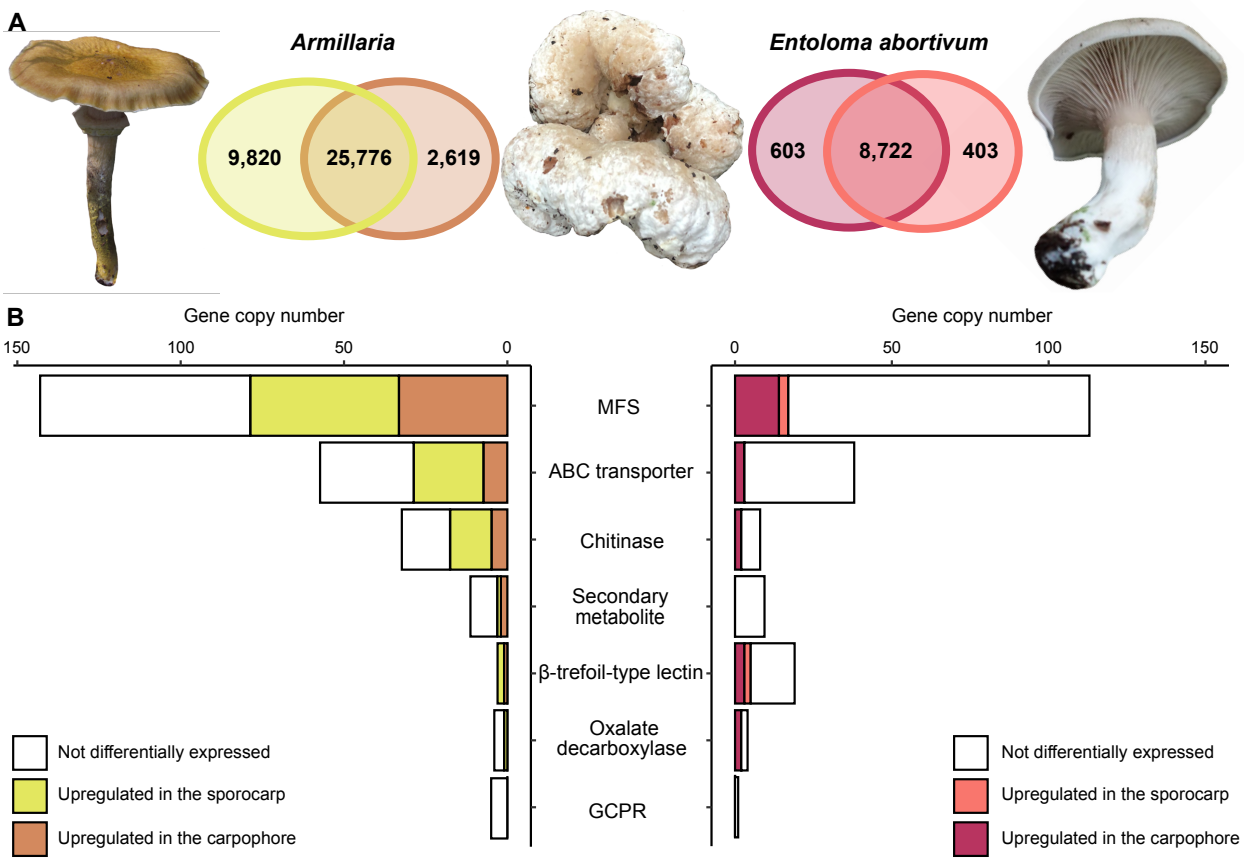

964

965 **FIG 3** Differentially expressed genes in the sporocarp and carpophoroid. (A) Venn
966 diagram showing the number of differentially expressed genes between the sporocarp
967 and carpophoroid in *Armillaria* and *E. abortivum*; photo of *E. abortivum* taken by Eva
968 Skific. (B) Bar graph showing the number of gene copies of genes important in
969 mycoparasitic interactions. The white portion of the bar shows the number of these
970 genes detected in the transcriptome but not differentially expressed, while the darker
971 colors (brown and purple, respectively) show the number of these genes that are
972 significantly upregulated by each species in the carpophoroid and the lighter colors
973 (yellow and coral, respectively) show the number of these genes that are significantly
974 upregulated by each species in their respective sporocarp.

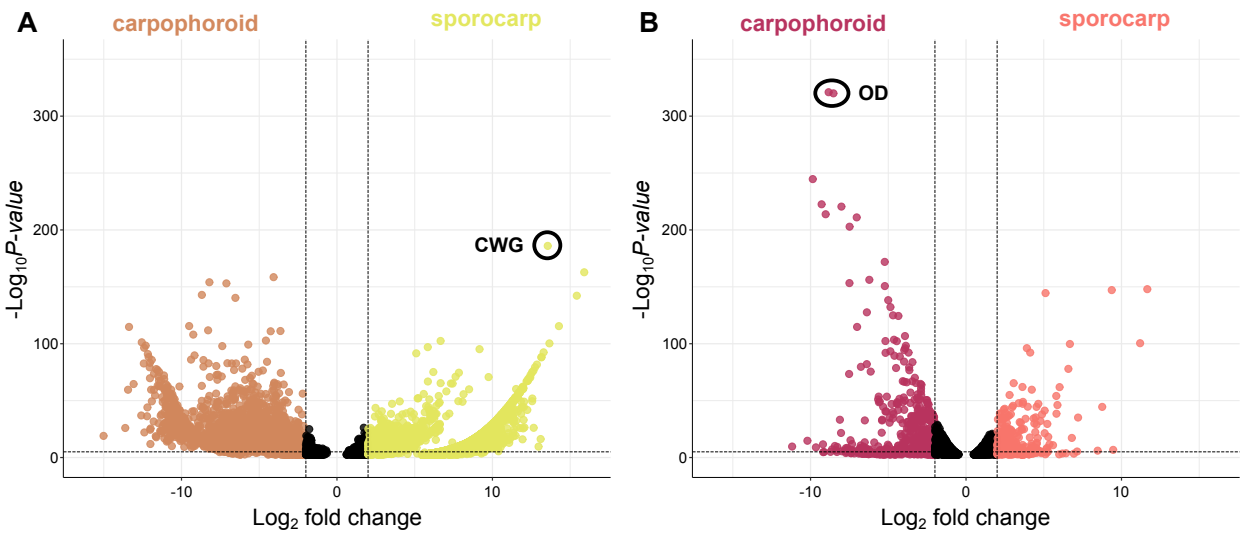

FIG 4 Volcano plots. Each dot represents a gene plotted according to its logFC and the -log10 of its *p*-value. All genes with a *q*-value < 0.05 are shown. Black dots represent a gene with a non-significant logFC (-2 < logFC < 2). (A) *Armillaria*. (B) *E. abortivum*. Dots with a black circle around them are annotated according to the abbreviations OD: oxalate decarboxylase; CWG: cell wall galactomannoprotein.

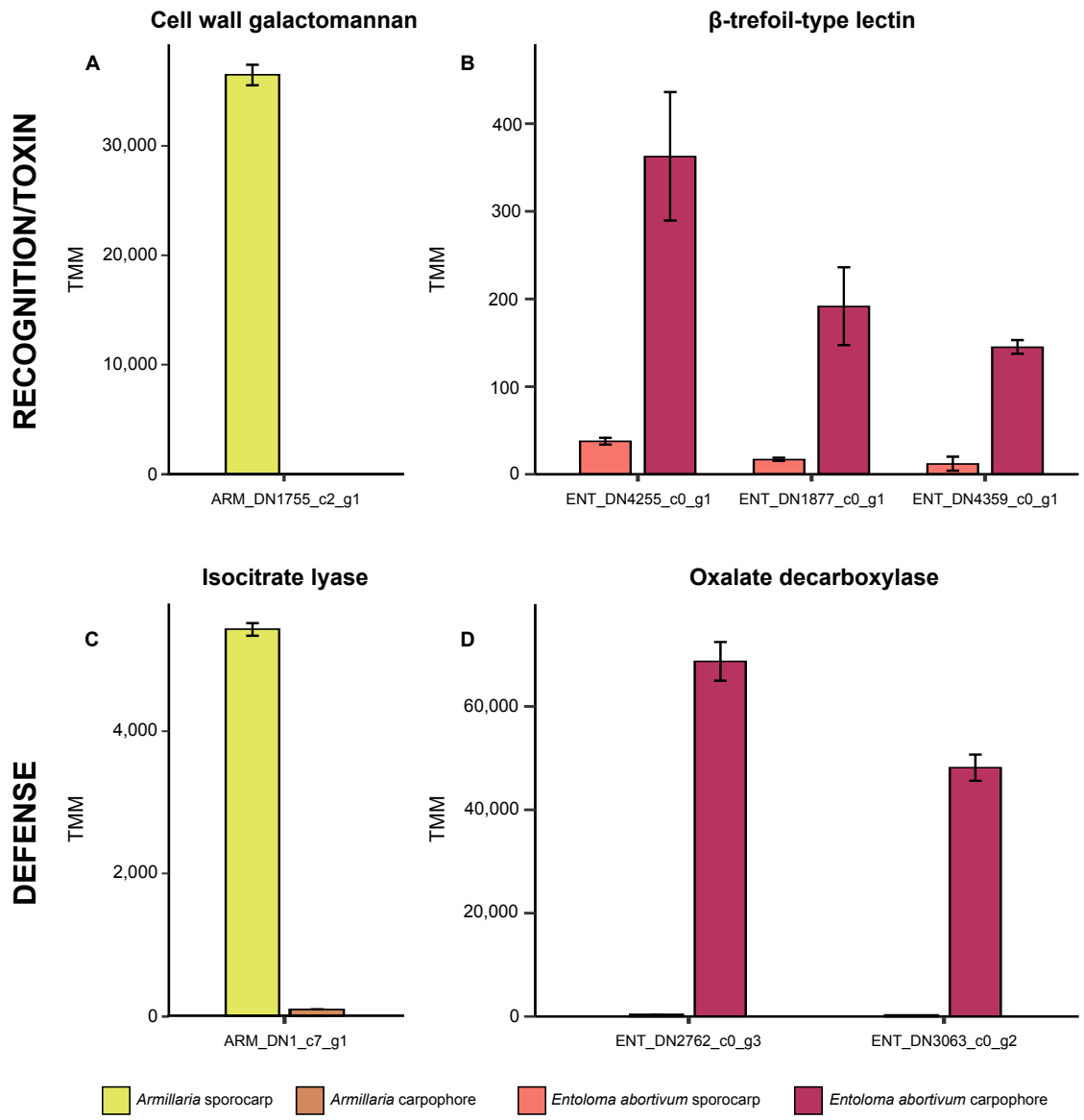

FIG 5 Genes in both *Armillaria* and *E. abortivum* that are putatively important in the recognition and defense responses during this mycoparasitic interaction. (A) One *Armillaria* cell wall galactomannan that is significantly upregulated in the sporocarp; (B) three *E. abortivum* β-trefoil-type lectins that are significantly upregulated in the carpophoroid; (C) one *Armillaria* gene that codes for isocitrate lyase that is significantly upregulated in their sporocarps; and (D) two *E. abortivum* genes that code for oxalate

989 decarboxylases that are significantly upregulated in the carpophoroids. All results are

990 shown as means ± standard error of the mean.

991

992

993

994

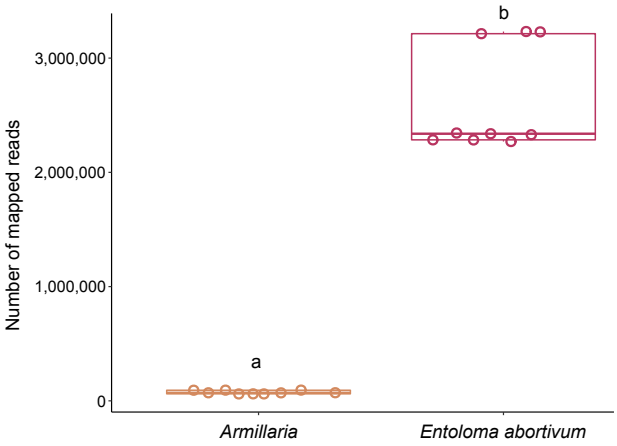

FIG 6 Boxplots of number of carpophoroid reads that mapped to *Armillaria* and *E. abortivum* when MAPQ = 30. Individual data points are indicated for each species with an open circle. The continuous line within each box represents the mean number of mapped reads. Species labeled with different letters (a to b) have a statistically significant ($p < 0.05$) different number of mapped reads in the carpophoroid.

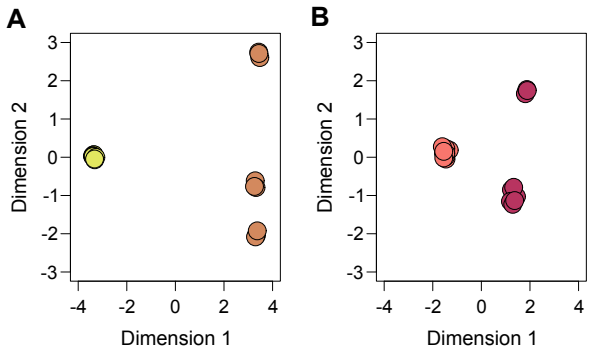

1004

1005 **FIG 7** Multidimensional scaling plot of distances between gene expression profiles for

1006 each sample. (A) *Armillaria* sporocarps and carpophoroids. (B) *E. abortivum* sporocarps

1007 and carpophoroids. For both figures, the lighter colors on the left represent the

1008 sporocarps, while the darker colors on the right represent the carpophoroids.

1009

1010

1011 **FIG 8** Phylogenetic placement of the *Armillaria* species used in this analysis. (A)
1012 Maximum likelihood phylogeny of *Armillaria* species and *Guyanagaster necrorhizus*
1013 generated from the analysis of 100 random BUSCOs. The outgroup taxon is
1014 *Cylindrobasidium torrendii*. Each node is fully supported with 100% bootstrap
1015 supported. (B) Maximum likelihood phylogeny of *Armillaria mellea* phylogenetic tree
1016 generated from the analysis of the ITS region. Branches with 70% or more bootstrap
1017 support are thickened. Outgroup taxa include *A. gemina, A. luteobubalina*, *A. puiggarii*
1018 and *A. sinapina*. The *Armillaria* specimen analyzed during this study is in bold and
1019 yellow in both phylogenies.
1020
1021